POLISH JOURNAL OF SOIL SCIENCE
VOL. LII/1 2019 PL ISSN 0079-2985

DOI: 10.17951/pjss/2019.52.1.75

ABDERZAK MOUSSOUNI*, MALEK BOUHADEF*, LIATIM MOUZAI*

NEW APPROACH TO ESTIMATE THE SHEAR STRESS AND THE FORCE OF RAINDROPS AND THEIR EFFECT ON ERODIBILITY OF AGRICULTURAL SOILS

Received:25.06.2018
Accepted:19.02.2019

Abstract. The objective of this work was to the study the erosive force of raindrops and the shear stress on the soil erodibility of disturbed and saturated agricultural soil. A mathematical development was used to determine a new approach to the shear stress. The soil erodibility is calculated using the WEPP (water erosion prediction project) model. To realize this work, an experimental study was led in a laboratory using the rainfall simulator. The soil tray used in this study has a length of 2 m, width of 50 cm and a depth of 15 cm and the slope was adjusted with a system. The soils used were sandy and silty agricultural soils. The results show that the relationship between the erosive force of raindrops and the shear stress on the soil erodibility increased respectively as a power and linear function with an important coefficient of determination. As regards the relationships between soil erodibility and the mean raindrop diameter, the evolution is represented by a power function with high coefficient of determination.

Keywords: erosive force, raindrops, rainfall simulator, shear stress, soil erodibility

1. INTRODUCTION

The problems of soil erosion became a major preoccupation of researchers in such fields as hydraulics, agronomics, ecology and economics. Ellison (1947) defines erosion as a complex phenomenon, resulting from the soil detachment by

* University of Sciences and Technology Houari Boumediene, Faculty of Civil Engineering, LEGHYD Laboratory, BP 32, Bab-Ezzouar, Algiers, Algeria. Authors' e-mails: amoussouni@usthb.dz; mbouhadef@usthb.dz; lmouzai@usthb.dz

the impact of raindrops and from the transport of particles removed by the surface flow. This phenomenon is mainly due to the parameters of rainfall erosivity and the parameters of resistance of the soil to erosion referred to as "erodibility". The erosive potential of the rain is indicated by the term "erosivity" (Bergsma *et al.* 1996). Rainfall erosivity is the capacity of the rain to cause erosion (Hudson 1995). There are several parameters of erosivity which cause soil erosion. The rain represents the most determining climatic factor of the soil erosion. The influence of the rain can be represented by the rainfall intensity, rainfall velocity, raindrops' erosive power (Shih and Yang 2009), report between the rainfall intensity and the flow depth (Ferro 1998). Hudson (1995) quoted that the rainfall intensity is particularly important as an erosivity parameter. The rainfall erosivity depends, on the one hand, on the rainfall intensity and, on the other hand, on the characteristics of raindrops as far as the size, the velocity, the form and the angle of impact are concerned (Riezebos and Epema 1985, Salles *et al.* 2000, Erpul *et al.* 2002). Zachar (1982) cited that the kinetic energy of raindrops is the basic factor when determining soil erosion. This size is important to know because it conditions the mechanical work made by the rain under the influence of the mass and the terminal velocity of raindrops. Bultot and Coppens (1985) indicated that the erosive power of rain is directly dependent on its power. The relationship between the mass and raindrops' diameter which free a kinetic energy with a raindrop fall velocity develop destructive aggregates under the name of erosive force of rain.

Some researchers consequently cited the erosive parameters of runoff. Ferro (1998) said that the shear stress or the tangential force exercised by the flow on the bed has an effect on the detachment and the transport of sediments. Govers *et al*. (1990) defined the soil detachment particles as the displacement of the soil particles in a particular place on the soil surface by the erosive force of the precipitation and the runoff, which can lead to the training of rill and gully. Bryan *et al*. (1989) quoted that various properties determine the soil erodibility for every under-erosion process and the erodibility can be defined only and exactly for identified processes and erosive strengths. The erodibility is the soil capacity to resist erosional processes (Bryan *et al*. 1989). The slope gradient is one of the factors affecting the runoff and the soil erosion. The quantity of soil eroded increases with the gradient of slope (Fox and Bryan 1999, Kinnell 2000). It depends essentially on the texture and the structure of the soil. Soil erodibility is also the soil capacity to resist a runoff force (Ozoko and Edeani 2015).

The objective of this study is to better understand the phenomenon of soil erosion, the influence of erosive forces of rainfall and runoff on agricultural soils' erodibility using the rainfall simulator. These forces depend on various erosive parameters like rainfall intensity, shear stress, raindrops' diameters, raindrop fall velocity, stream velocity and flow sediments. The soil erodibility was estimated using the WEPP model. It can be accurately estimated only by defined wrenching and drive forces which affect soil.

2. THEORETICAL APPROACH

2.1. Erosive rainfall force

The force of raindrops is the combination of the characteristics of raindrops such as the mass, the velocity and the raindrops' diameter. Mouzai and Bouhadef (2003) quoted that this combination shows the extent to which the mass, the velocity and the raindrops' diameter affect the detachment and the transport of sediments. This strength was defined by Riezebos and Epema (1985) using the following formula:

$$F = \frac{M V^2}{d} \quad (1)$$

Where: *M* (kg) is the mass of raindrops, *V* ($m \cdot s^{-1}$) is the raindrops fall velocity and *d* (m) is the raindrops' diameter.

Using the median diameter of raindrops the relation (1) becomes:

$$F = \frac{M V^2}{d_{50}} \quad (2)$$

Where: d_{50} is the median raindrop diameter (mm).

For measuring the raindrop diameter, we used the stain method or method of absorbent paper (Hudson 1995). This method is based on the principle that the falling drop on a uniform absorbent surface produces a stain the diameter of which is proportional to the diameter of the raindrop. For our experiments, we used absorbent paper with potassium permanganate powder ($KMnO_4$) which is a dye which changes the color when it gets wet and becomes mauve.

The treated paper is placed on a glass plate of the same size and is held horizontally, covered with another glass plate of a larger size. The paper is then simply submitted, at a very short time, to the simulated rain and when the sheet is dry, the impact of raindrop appears mauve. A magnifying glass to measure the impact diameter was used. The number of drops varies from one sheet to another depending on the rainfall intensity. Then we determine the raindrops' median diameter.

The relation between the median diameter (d_{50}) and the rainfall intensity (I) is represented in Moussouni *et al*. (2012) by the following power formula:

$$d_{50} = 0.945\, I^{0.245} \quad (3)$$

Where: *I* ($mm \cdot h^{-1}$) is the rainfall intensity and d_{50} (mm) is the median raindrop diameter.

The raindrop fall velocity depends on its mass, thus, on its diameter. It increases during the fall to reach a limit velocity or a terminal velocity.

Schmidt (1993) cited in Shih and Yang (2009), gave the relation of the raindrops' fall velocity according to the rainfall intensity by the following relation:

$$V = 6.6\, I^{0.07} \tag{4}$$

2.2. Shear stress

Rauws and Govers (1988) and Torri *et al*. (1987) showed in their studies on soil erosion mechanics that the condition at which rill flow becomes erosive is controlled by soil surface shear strength (Brunori *et al*. 1989). Besides, Nearing and Bradford (1985) quoted that splash detachment processes are strictly linked to soil shear strength (Brunori *et al*. 1989).

In the case of a flow generated by rainfall on a saturated no cohesive soil, the difference of the total load between two sections of a distance *dx* is equal to losses due to the friction force. This equation is mentioned by Graf and Altinakar (2000):

$$d\left(z + h + \frac{U^2}{2g}\right) = \frac{1}{g}\frac{\tau}{\rho_{mix}}\frac{dp}{dA}dx \tag{5}$$

Where: *p* is the wet perimeter (m), *A* is the wet section (m^2), ρ_{mix} is the density of the mixture water-sediments ($kg{\cdot}m^{-3}$), *z* is the soil elevation (m), *g* is the gravity ($m{\cdot}s^{-2}$), *h* is the flow depth (m), *U* is the flow velocity ($m{\cdot}s^{-1}$), *x* is the flow length (m) and τ is the shear stress or the tractive force of particles.

The item $d\left(z + h + \frac{U^2}{2g}\right)$ is only the energy by the unit mass. This energy changes along the soil because of the changes of bottom height and the energy losses.

In the case of a flow of a disturbed agricultural soil, the variation of the flow velocity is negligible in front of the depth. The equation (5) becomes, by dividing on *dx*:

$$\frac{d}{dx}(z + h) = \frac{1}{g}\frac{\tau}{\rho_{mix}}\frac{dp}{dA} \tag{6}$$

$\frac{dz}{dx}$ is the soil slope.

To determine the variation of the depth $\frac{dh}{dx}$ we leave the unidimensional equation of continuity which is based on the principle of the determination of rate sediments detachment during the precipitation and requires prediction of slope variation and flow depth. This slope variation and flow depth are determined by approximation of the flow kinetics, which implies that the surface slope of the flow is parallel to the slope gradient. For a flat slope, the following equation is provided:

$$U\frac{q_e}{\partial x}+\frac{\partial h}{\partial t}=I(t)-f(t) \tag{7}$$

Where: q_e is the streaming water flow by width unity ($m^2 \cdot s^{-1}$), h is the flow depth (m), I is the rainfall intensity ($m \cdot s^{-1}$) and f is the infiltration capacity.

In the case of a saturated soil and when the rainfall intensity is constant with the time t, the equation (7) becomes:

$$\frac{q_e}{\partial x}=I \tag{8}$$

After integration, the equation (8) becomes:

$$q_e = Ix \tag{9}$$

Several researchers, for example, Abrahams *et al*. (2001) represented the flow of water-sediment mixture, by the following formula:

$$q_{mix} = q_e + q_s \tag{10}$$

From which:

$$q_{mix} = Ix + q_s \tag{11}$$

Where: I is the rainfall intensity ($m \cdot s^{-1}$), x (m) is the streaming length, q_{mix} is the flow of water-sediment mixture by width unity, q_e is the liquid volume flow by width unity ($m^2 \cdot s^{-1}$), q_s is the solid volume flow by width unity ($m^2 \cdot s^{-1}$).

The variation of the flow of water-sediments mixture according to the distance can be written in the following form (Kinnell 1993, Kinnell 1991):

$$q_{mix} = Uh \tag{12}$$

The derivative of the equations (11) and (12) in relation to the length x and the equality of this equation gives:

$$U\frac{dU}{dx}+U\frac{dh}{dx}=I+\frac{d\,q_s}{dx} \tag{13}$$

The equations (6) and (13) become:

$$U\frac{dh}{dx}=I+\frac{d\,q_s}{dx} \tag{14}$$

$$\frac{dh}{dx}+\frac{dz}{dx}=\frac{1}{g}\frac{\tau}{\rho_{mix}}\frac{dp}{dA} \tag{15}$$

The combination of the equations (14) and (15) becomes:

$$\frac{I}{U} + \frac{d\,q_s}{U\,dx} + S = \frac{1}{g}\frac{\tau}{\rho_{mix}}\frac{dp}{dA} \tag{16}$$

For a rectangular section with width *b* (m), the wet perimeter dP = b+2h and the wet section dA = bh. The report $\frac{dp}{dA} = \frac{2}{b}$

The equation (16) becomes:

$$\frac{d\,q_s}{dx} = \frac{U}{g}\frac{\tau}{\rho_{mix}}\frac{2}{b} - I - US \tag{17}$$

After integration we have:

$$\tau = \frac{(q_s \quad +I\,x+U\,S\,x)\,g\,b\,\rho_{mix}}{2\,U\,x} \tag{18}$$

With τ is the shear stress (kg·m^{-1}·s^{-2}).

The density of the water-sediment mixture is defined by the following relation:

$$\rho_{mix} = \frac{m_{mix}}{W_{mix}} = \frac{m_e \quad +m_s}{W_e \quad +W_s} \tag{19}$$

Where: m_e is the mass of water, m_s is the mass of sediments, m_{mix} is the mixture mass of water/sediment, W_e is the volume of water, W_s is the volume of sediments and W_{mix} is the volume of water-sediment mixture.

The equation (19) becomes:

$$\rho_{mix} = \frac{\rho_s\,m_e + \rho_s\,m_s}{W_e + W_s}$$

From which we will have:

$$\rho_{mix} = \rho_e \frac{W_e}{W_e \quad +W_s} + \rho_s \frac{W_s}{W_e + W_s} \tag{20}$$

The sediments concentration was defined as the ratio between the dry weight of sediment and the runoff volume (Guy *et al*. 1990, Abrahams and Atkinson 1993):

$$C_s = \frac{m_s}{W_t} = \frac{m_s}{W_e + W_s} \tag{21}$$

Or:

$$C_s = \rho_s \frac{W_s}{W_e + W_s} \tag{22}$$

The density of the water-sediments mixture can be written by the following relation:

$$\rho_{mix} = \rho_e + \left(1 - \frac{\rho_e}{\rho_s}\right) C_s \quad (23)$$

Where: Cs is the sediments concentration (kg·m^{-3}).

2.3. Soil erodibility

In the WEPP (Water Erosion Prediction Project) model, interrill surfaces erosion is expressed as (Kinnell and Cummings 1993):

$$E = K\, I^2\, S_f \quad (24)$$

Where: E is the interrill erosion rate (mass of soil eroded per area unit per time unit), K is the soil erodibility, I is the rainfall intensity and S_f is the slope factor, which is expressed by the equation (Truman and Bradford 1993, Kinnell 1993):

$$S_f = 1.05 - 0.85\, e^{-4\sin\theta} \quad (25)$$

Where: θ is the slope angle.

Kinnell (1993) quoted the equation that connects the interrill erosion rate with the solid flow by the relation:

$$E = \frac{q_s}{x} \quad (26)$$

Where: x is the length of the surface affected in the flow direction.

The combination of the equations (24) and (26) gives the expression of the erodibility as follows:

$$K = \frac{q_s}{x\, I^2\, S_f} \quad (27)$$

With K is the soil erodibility (kg·s·m^{-4}).

Dividing the numerator and denominator of the equation (21) by the width and time, becomes:

$$C_s = \frac{q_s}{q_{mix}} \quad (28)$$

Where: q_s is the unit solid discharge (kg·m^{-1}·s^{-1}), q_{mix} is the unit mixture discharge (m^2·s^{-1}) and C_s is the sediments' concentration. Replacing equation (28) with equation (27) becomes:

$$K = \frac{q_{mix}\, C_s}{x\, I^2\, S_f} \quad (29)$$

3. EXPERIMENTAL PROCEDURE

3.1. Rainfall simulator

The simulator which is used is an ORSTOM type with a spray nozzle fixed on a gantry at a height of about three meters on the soil tray, livened up by a pendulum movement of such manners to cover the soil surface. The nozzle sprinkles a surface test of 1 m^2. This system includes a motor provided with an arm serving to assure the oscillation. The nozzle is supplied with water by a pipe, which, in turn, is connected with a tank. To change the rainfall intensity, a control valve is installed on the discharge pipe; a manometer, placed before the nozzle, allows indicating pressure corresponding to each rainfall intensity. The carriage allows placing the cover in order to protect the parcel from the wind. This type of rainfall simulator is used, *inter alia*, by Moussouni *et al.* (2012).

3.2. Soil tray

The tray is made of Plexiglas. It is similar to the one used by, for example, Abrahams and Atkinson (1993) during their study on the relation between the velocity of grain and the sediments concentration in the surface flow. The soil tray has a length of 2 m, width of 0.5 m and a depth of 0.15 m. It is fixed on a metallic frame serving as a support. On one end of this support is fixed an axis which allows the tray to pivot. On the other end, it is lifted *via* two threaded rods, provided with flywheels, to fix the desired inclination of the tray. A collector of liquid solid flow is fixed to the outlet of the tray with an inclined bottom in order to avoid the decantation of the solid particles.

3.3. Soil preparation

The soils material used to run the experiments was an agricultural soil which had been examined for stones and roots which were removed in order to have a homogenous structure. The results of physical analyses of soils are provided in Table 1.

To run an experiment, a layer of examined soil was deposited and spread gently over the surface tray. To obtain a flat plot, in the purpose to generate a flat sheet of water, a straight piece of hardwood was used to flatten the surface until the top soil is at the level of the bottom end of the tray. Afterwards, the soil was wetted gently without disturbing the soil structure, with a watering can (fine rain) until saturation (Pan and Shangguan 2006). This operation was made on a flat surface. Then the rainfall simulator is put on to run the experiment. When the soil is saturated, we fixed the slope angle of the soil tray at 3%, 4%, 5% and 7% which amounts respectively to 1.7°, 2.3°, 2.9°, 4° and is appropriate for generating an interrill flow. These slopes represent average slopes of the plots of technical institute of market gardening and industrial. This method was already used by Bryan (1976, 1979) and Collinet and Valentin (1984). The application of the simulated rain is realized as soon as the slope is fixed so that the soil does not lose water caused by the slope. When the water wave is established, the measurements are taken.

Table 1. Physical analysis of soil

Sample	Clay	Fine silt	Coarse silt	Fine sand	Coarse sand	Organic matter
Silty soil (%)	17.80	26.50	36.75	10.50	8.45	1.92
Sandy soil (%)	3.55	13.35	20.36	23.30	39.44	2.57

3.4. Measure of the rainfall intensity

The procedure used to measure the rainfall intensities is the volumetric method. The measurement is taken by means of a gate installed on the conduct of expulsion and by the speed of oscillation of the pendulum. For this, we placed beakers, spread uniformly on the entire surface of the flume soil. This method has been already used by Moussouni *et al*. (2012). The volume of water collected in every beaker was measured by means of a gradual test tube. This volume is divided by the duration and the beaker surface. This handling is repeated five times with the calculation of the uniformity coefficient in order to receive mean rainfall intensities. The rainfall intensities used in this study are: 102 $mm \cdot h^{-1}$; 90 $mm \cdot h^{-1}$; 73 $mm \cdot h^{-1}$; 66 $mm \cdot h^{-1}$; 38 $mm \cdot h^{-1}$ and 28 $mm \cdot h^{-1}$.

3.5. Surface velocity measurement

The method used to measure the surface velocity (U_s) is the same as the one used by several authors (Guy *et al*. 1990, Farenhorst and Bryan 1995, Li 2009, Gimenez and Govers 2002, Pan and Shangguan 2006, Maaliou and Mouzai 2018). This method is based on using potassium permanganate ($KMnO_4$) as a dye tracer. The surface velocity was measured by tracing the traveling time of dyes over the distance specified according to the soil tray dimensions. Wherever this tray is divided into sections of 50 cm, the measure marks are fixed. The distance is limited from 0.5 m to 2.0 m; four positions (0.5 m, 1 m, 1.5 m and 2 m) were selected to record the travelling time of the leading edge in order to get a uniform flow avoiding the effects of the top edge of the surface flow. To avoid the effects of the rain impact on the dye tracing, potassium permanganate powder is used. The colored liquid is injected at the head of the soil tray. Surface flow velocities were then measured visually by recording the time of the leading edge of the dye cloud travelling between the injection point and 2.0 m bottom end of the soil tray. The mean flow velocity U is calculated from the surface velocity U_s using the conversion factor of 0.67 (Li 2009).

The surface velocity measured is equal to the distance covered *x* by the travels time *t*:

$$U_S = \frac{x}{t} \tag{30}$$

The mean flow velocity is equal in:

$$U = 0.67U \tag{31}$$

3.6. Flow sediments concentration measurement

The discharge *Q* was measured volumetrically. Determined from the rate of water-sediment mixture volume W_{mix} and time *t* using $Q = \frac{W_{mix}}{t}$. The volume of the water-sediment mixture is measured in the output collector. The stream flow begins just after the rain reaches the soil, it is due to the initial saturation of the soil and the measurement is taken in the first minute. The water volume collected in each beaker was measured using a graduated cylinder of 1,000 ml for the time of 30 seconds; this operation is reproduced every 3 minutes until the end of the test (Fox and Bryan 1999, Bryan and Brun 1999). Thereafter, the beaker is stirred so that all the solids particles are suspended in water; we take a sample of 100 ml in a small glass beaker which we measured previously the empty weight (Pan and Shangguan 2006). Having noted the volumes of all the beakers and collected after cleared volumes of 100 ml of the mixture, we put these glass beakers in the oven at a temperature of 105°C for 24 hours (Fox and Bryan 1999).

After 24 hours, we weight the beakers with dry sediments to obtain the mass of sediments in 100 ml from some mixture (Pan and Shangguan 2006). The difference between the weights of empty and filled beakers gave the mass of sediments in $kg \cdot m^{-3}$.

3.7. Mean flow depth

Mean flow depth is an important factor of the surface flow, but it is very difficult to determine, because of the soil erosion process. Pan and Shangguan (2006) and Guy *et al*. (1990) used the *h* equation (12) $h = \frac{q_{mix}}{U}$ to calculate the mean flow depth, where q_{mix} is the mixed overland flow discharge and *U* is the mean velocity.

4. RESULTS AND DISCUSSION

4.1 Erosive raindrop force

Our results show that the impact of the erosive force on the soil erodibility is connected with the raindrop diameter and the raindrop fall velocity by the equations (3) and (4). The detachment rate by the splash is linked to the raindrop kinetic energy, the type of soil and the size of raindrops (De Ploey and Savat 1968). In this study the raindrops diameter varied between 2.138 and 2.935 mm for rainfall intensities from 28 to 102 $mm \cdot h^{-1}$. These raindrops diameters and their impact bear the greatest responsibility for the erosion rate, soil particle detachment and the splashing of the detached particles. Mouzai and Bouhadef (2003) mentioned that when raindrops hit the bare sandy soil, the droplets appear and divide into several droplets of different sizes. Sets of droplets were splashed out carrying soil particles. The quantity of these particles depends on the droplet's characteristics such as diameter, volume, transport capacity and the arrangement of particles. The impact of raindrops is visible in decomposition of the aggregates, detachment of the particle from the soil surface, and the transport of these particles in random directions (Leguédois *et al*. 2005).

The relationships between the median raindrop diameter and the soil erodibility for the various slopes and for both types of soil are presented in Figures 1 and 2.

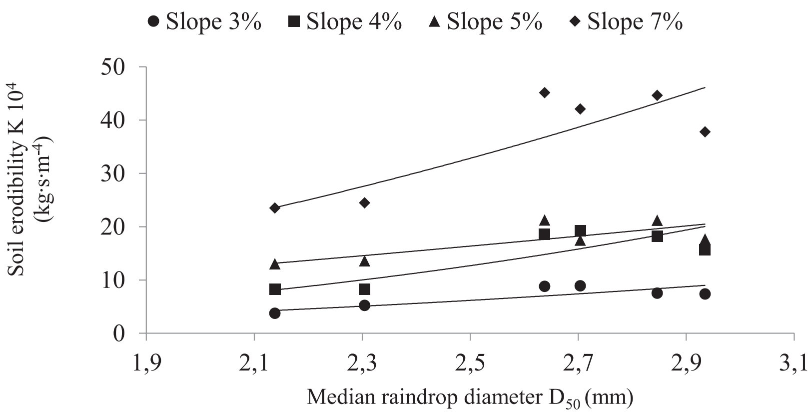

Fig. 1. Relation between soil erodibility and the raindrops median diameter of a silty soil

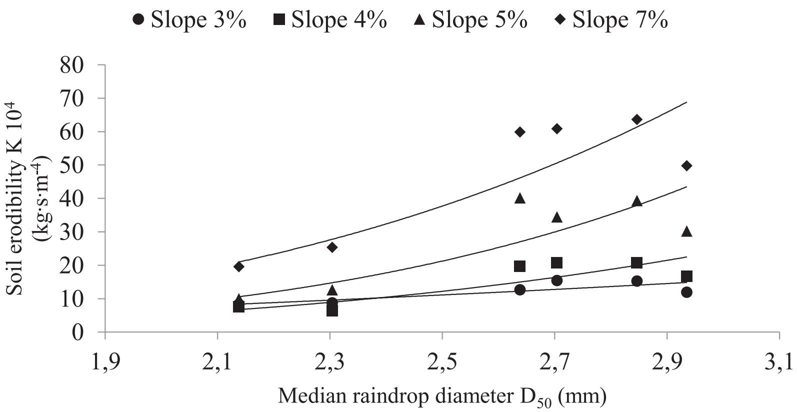

Fig. 2. Relation between soil erodibility and the raindrops median diameter of a sandy soil

The functions and the determination coefficients which govern the soil erodibility and the median raindrops diameter are provided in Table 2.

Table 2. Functions and determination coefficients of the soil erodibility and the median raindrops diameter

Soil type	Silty soil		Sandy soil	
Slope (%)	Function (K 10^4)	R^2	Function (K 10^4)	R^2
3	$K = 0.72\ D_{50}^{2.35}$	0.77	$K = 2.12\ D_{50}^{1.81}$	0.72
4	$K = 0.93\ D_{50}^{2.85}$	0.73	$K = 0.37\ D_{50}^{3.81}$	0.76
5	$K = 4.52\ D_{50}^{1.40}$	0.75	$K = 0.36\ D_{50}^{4.47}$	0.82
7	$K = 4.71\ D_{50}^{2.12}$	0.71	$K = 1.21\ D_{50}^{3.75}$	0.83

For all the range of the rain intensity, the soil erodibility increases with the increasing slope. For intensity going from 28 to 102 $mm{\cdot}h^{-1}$ and for slope angles going from 3% to 7%, the correlation is significant, ranged from 0.71 to 0.77 for a silty soil and from 0.72 to 0.83 for a sandy soil. The function follows well the power law.

The detachment of particles influenced by the raindrops diameter is much more important for a sandy soil than a silty one. It is certainly due to the soil texture. Diaz Zorita *et al.* (2002) indicated that the soil erodibility is related to the structural stability. Silty soils have a low cohesion and contain very small particles. Thus, they are easily removed from the soil matrix and easily transported. Fine sands have an even lower cohesion. Coarse sands have a very low cohesion, but because they are sediments bigger than silt and fine sands, they are less easily transported by runoff water. In our case the size of sediments did not influence the transport of sediments by runoff.

The combination impact of the mass and the fall velocity of raindrops are transformed, when they contact the soil surface, in erosive force of raindrops which remove and splash the soil particles. Figures 3 and 4 show the effect of the erosive force of raindrops on the soil erodibility for the various slopes.

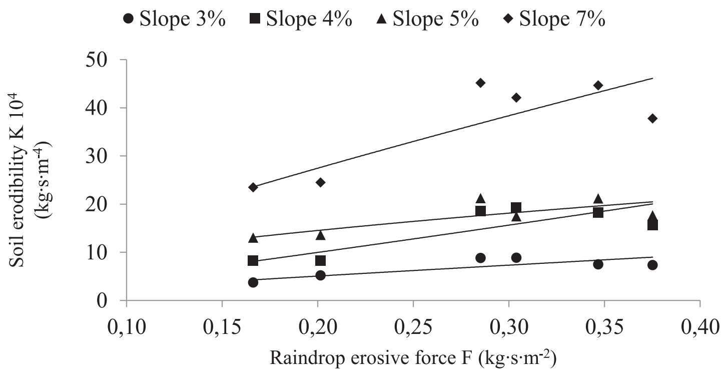

Fig. 3. Relation between the erosive force of raindrops and the soil erodibility of a silty soil

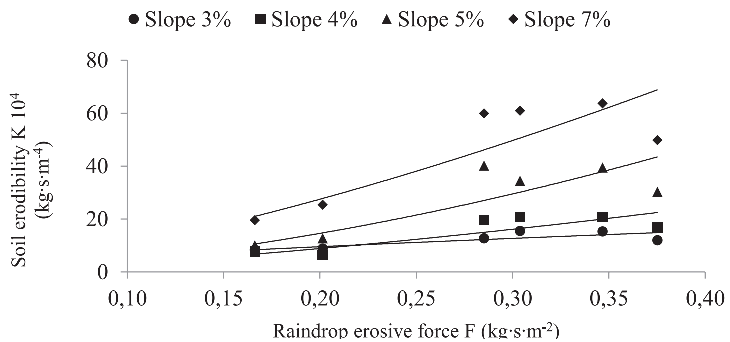

Fig. 4. Relation between the erosive force of raindrops and the soil erodibility of a sandy soil

The functions and the determination coefficients are illustrated in Table 3.

Table 3. Functions and determination coefficients of the soil erodibility according to the erosive force of raindrops

Soil type	Silty soil		Sandy soil	
Slope (%)	Function (K 10^4)	R^2	Function (K 10^4)	R^2
3	$K = 20.94\ F^{0.89}$	0.77	$K = 29.53\ F^{0.70}$	0.72
4	$K = 62.78\ F^{1.14}$	0.77	$K = 95.94\ F^{1.48}$	0.76
5	$K = 34.93\ F^{0.55}$	0.69	$K = 238.4\ F^{1.74}$	0.82
7	$K = 91.20\ F^{0.75}$	0.71	$K = 287.5\ F^{1.46}$	0.83

The estimation of soil erodibility depends on the mixture of water and sediments, the sediments' concentration, the rain intensity, the eroded length surface and slope factor. According to the results presented above, we report which functions follow well the power law with a significant coefficient of determination. When the erosive force of raindrops increases, the soil erodibility increases as well: for a silty soil, from 7.36 10^4 kg·s·m^{-4} to 37.78 10^4 kg·s·m^{-4} and for a sandy soil of 11.93 10^4 kg·s·m^{-4} to 49.80 10^4 kg·s·m^{-4} corresponding to the slope angles from 3% to 7% under the rain intensity of 102 mm·h^{-1}. The increase of the soil erodibility in our study is also registered with all the rainfall intensity going from 28 to 102 mm·h^{-1}. We notice in this case that the effect of the erosive force of raindrops is more important for a sandy soil than a silty one.

The values of this study are confirmed by the values measured by Romero *et al*. (2007) where they give range values of 1.9 10^5 kg·s·m^{-4} to 56 10^5 kg·s·m^{-4} with an angle of natural inclination and the rainfall intensities from 7.5 to 150 mm·h^{-1}. This last intensity (150 mm·h^{-1}) has a shorter duration. They indicated that most of the eroded soils are the ones which contain the highest amount of silt and fine sands and the most resistant are the clay soil. The silt and sand are strongly correlated to the values of the soil erodibility.

4.2 Shear stress

The relation (18) shows that at the same time the shear stress depends on solid flow, the rainfall intensity, the flow velocity, the density of water-sediments mixture, slope factor, the length and the width of the soil tray. The influence of shear stress on the soil detachment particles involves the influence of all these runoff parameters. The results obtained in this study for various slopes and for various rainfall intensities are represented in Figures 5–8.

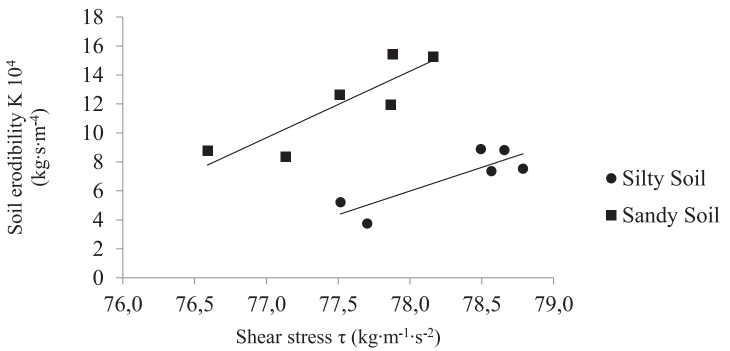

Fig. 5. Relation between the soil erodibility and the shear stress for a slope angle of 3%

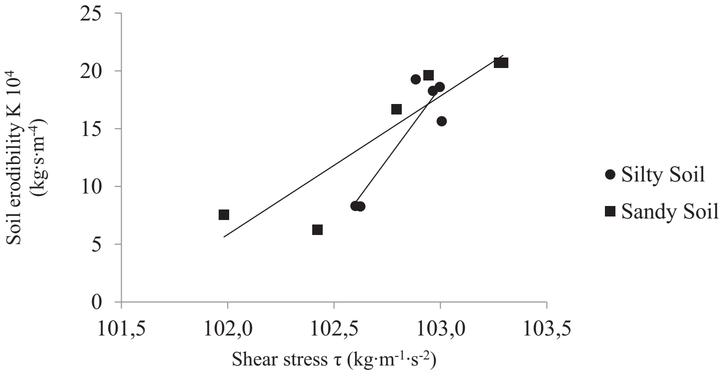

Fig. 6. Relation between the soil erodibility and the shear stress for a slope angle of 4%

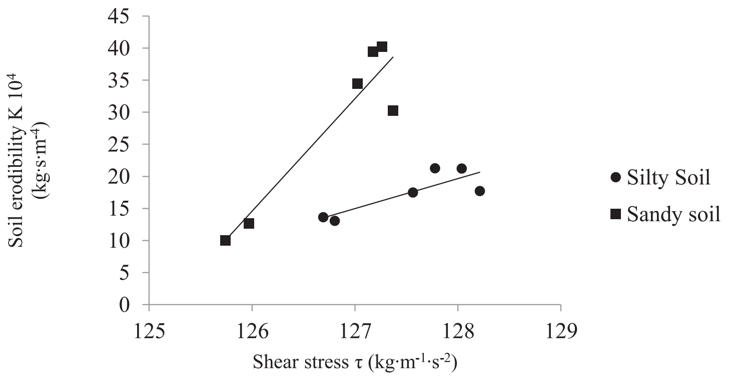

Fig. 7. Relation between the soil erodibility and the shear stress for a slope angle of 5%

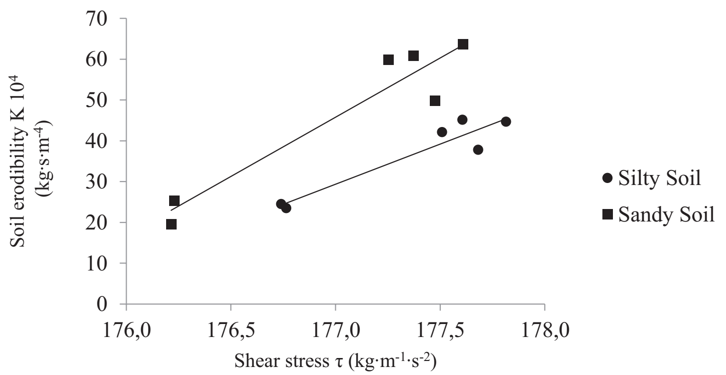

Fig. 8. Relation between the soil erodibility and the shear stress for a slope angle of 7%

We notice that the relation which concerned the shear stress with the soil erodibility follows well a linear law with significant coefficients of determination. The laws of regression and the coefficient of correlation are provided in Table 4.

Table 4. Functions and determination coefficients of the soil erodibility according to the shear stress

Soil type	Silty soil		Sandy soil	
Slope (%)	Function (K 10^4)	R^2	Function (K 10^4)	R^2
3	$K = 3.26\tau - 248.6$	0.73	$K = 4.59\tau - 344.1$	0.76
4	$K = 24.96\tau - 2553$	0.82	$K = 11.98\tau - 1216$	0.85
5	$K = 4.67\tau - 578.5$	0.7	$K = 17.55\tau - 2197$	0.88
7	$K = 19.65\tau - 3449$	0.9	$K = 29.02\tau - 5090$	0.91

The results presented in Table 4 and illustrated in Figures 5–8 show that the shear stress has a significant influence on the soil erodibility. This effect is certainly connected, on the one hand, with the solid flow and the rainfall intensity which detached and transported the particles and, on the other hand, with the flow velocity which shears the soil particles along the streaming length.

The flow velocity varies from 0.01 $m \cdot s^{-1}$ to 0.032 $m \cdot s^{-1}$ corresponding with the intensities varying from 28 $mm \cdot h^{-1}$ to 102 $mm \cdot h^{-1}$ respectively with the slope angle of 3%. The flow velocity with the other slope angles of 4%, 5% and 7% develops in the same way with all the rainfall intensities. This evolution of the velocity was induced by the increase of the rainfall intensities.

Among the variables which also influence the shear velocity, there is a flow depth. The increase of the flow depth, which is due to the increase of the rainfall intensity, accentuates the flow velocity and gives the flow a high power to detach the surface soil particles and, consequently, the initiation of rill. This is confirmed by Govers (1985) and Rauws (1987).

Therefore, we can say that the rainfall intensity is the most dominant parameter and most influencing the soil erodibility. It influences the sediments concentration, which, in turn, influences soil erodibility. For a slope angle of 3% and rainfall intensities going from 28 to 102 $mm \cdot h^{-1}$, a sediments concentration varied respectively between 0.37 and 2.86 $kg \cdot m^{-3}$ for a silty soil and between 0.34 and 3.76 $kg \cdot m^{-3}$ for a sandy soil. The sediments concentration with the slope angles of 4%, 5% and 7% evolves in the same way with all the rain intensities. These results are confirmed by the conclusions of Kilinc and Richardson (1973). When studying the mechanics of the soil erosion, they used four rainfall intensities on sandy soil and six slopes angles (5.7%, 10%, 15%, 20%, 30%, and 40%). They found that the sediment concentration increases with increasing rainfall intensity for each slope.

We can indicate that the shear stress varied slightly with the variation of the rainfall intensity. For intensities ranged from 28 $mm \cdot h^{-1}$ and 102 $mm \cdot h^{-1}$, the shear stress varied respectively 77.7 $kg \cdot m^{-1} \cdot s^{-2}$ and 78.57 $kg \cdot m^{-1} \cdot s^{-2}$ for the silty soil, and between 77.13 $kg \cdot m^{-1} \cdot s^{-2}$ and 77.87 $kg \cdot m^{-1} \cdot s^{-2}$ for the sandy soil. It is practically constant for the various intensities and for the different types of soil. On the other hand, the variation of the shear stress is very significant when the soil slope varied. For silty soil, the slope angle of 3% and an intensity of 102 $mm \cdot h^{-1}$, the shear stress equals 78.57 $kg{\cdot}m^{-1}{\cdot}s^{-2}$, for the same intensity and the slope angle of 4%, the shear stress equals 103 $kg{\cdot}m^{-1}{\cdot}s^{-2}$, changes into 128 $kg{\cdot}m^{-1}{\cdot}s^{-2}$ for a slope angle of 5% and into 178 $kg{\cdot}m^{-1}{\cdot}s^{-2}$ for a slope angle of 7%.

5. CONCLUSIONS

Our objective was to understand the effect of the erosive force of raindrops and shear stress on the soil characteristics (soil erodibility, K). The effect of soil erodibility is sometimes studied by varying the slope with a fixed rainfall intensity and *vice versa*. We obtained interesting results:

Soil erodibility is influenced by the raindrop erosive force and the shear stress. The impact which is made by the raindrop erosive force is essentially due to the raindrops diameters and the velocity of falling raindrops. We noticed that when the raindrops' diameter varied from 2.14 mm to 2.94 mm for rainfall intensities going respectively 28 $mm{\cdot}h^{-1}$ at 102 $mm{\cdot}h^{-1}$, the raindrops erosive force varied from 0.17 $kg{\cdot}m{\cdot}s^{-2}$ to 0.38 $kg{\cdot}m{\cdot}s^{-2}$ and the soil erodibility passes from 3.75 10^4 $kg{\cdot}s{\cdot}m^{-4}$ to 7.36 10^4 $kg{\cdot}s{\cdot}m^{-4}$ under a slope angle of 3%. These results develop in the same way with all the slopes degrees.

The influence of the shear stress is due to the combination of runoff hydraulic parameters such as the solid flow, the flow velocity, the density of mixture water sediments and the slope factor. We concluded that this size varies lightly with the rainfall intensities and evolves with the evolution of the slope degrees. For a rainfall intensity of 102 $mm{\cdot}h^{-1}$, the shear stress is 78.57 $kg{\cdot}m^{-1}{\cdot}s^{-2}$ for a slope angle of 3%, this value changes into 178 $kg{\cdot}m^{-1}{\cdot}s^{-2}$ under a slope angle of 7%. We found out that the influence of shear stress is due to the increase of the flow depth, which is due to the increase of the rainfall intensity, accentuates the shear velocity and gives the flow a high power to detach soil surface particles. It is indicated that certain researchers neglect the influence of the parameters of streaming on the soil erodibility. Young and Wiersma (1973) analyzed the relative importance of the raindrops impact with regard to the influence of water on three various soil textures. Their study shows that the raindrops impacts are the main cause of the soil disintegration, whereas the flow transports the already detached particles. Bryan and Shiu-Hung (1981) show that the soil disintegration is due to the wash loss and splash loss.

We can mention that in the case of low slope, soil erodibility is due to particle-size distribution. We noticed that the sandy soil is more affected as compared to the silty soil. For a slope angle of 3%, the soil erodibility of sandy soil varied between 8.35 $kg{\cdot}s{\cdot}m^{-4}$ and 11.93 $kg{\cdot}s{\cdot}m^{-4}$ under rainfall intensities 28 $mm{\cdot}h^{-1}$ and 102 $mm{\cdot}h^{-1}$, respectively. On the other hand, for a silty soil, the variation is from 3.75 $kg{\cdot}m^{-4}$ to 7.36 $kg{\cdot}m^{-4}$. This is demonstrated by the fact that the size of aggregates is different for both soils.

REFERENCES

[1] Abrahams, A.D., Li, G., Krishnan, C., Atkinson, J.F., 2001. *A sediment transport equation for interrill overland flow on rough surfaces*. Earth Surface Processes and Landforms, 26(13): 1443–1459.

[2] Abrahams, A.D., Atkinson, J.F., 1993. *Relation between grain velocity and sediment concentration in overland flows*. Water Resources Research, 29(9): 3021–3028.

[3] Bergsma, E., Charman, P., Gibbons, F., Hurni, H., Moldenhauer, W.C., Panichapong, S., 1996. *Terminology for soil erosion and conservation*. ISSS.

[4] Brunori, F., Penzo, M.C., Torri, D.F., 1989. *Soil shear strength: Its measurement and soil detachability*. CATENA, 16: 59–71.

[5] Bryan, B., 1976. *Considerations on soil erodibility indices and sheetwash*. CATENA, 3: 99–11.

[6] Bryan, B., 1979. *The influence of slope angle on soil entrainment by sheetwash and rainsplash*. Earth Surface Processes, 4: 43–58.

[7] Bryan, R.B., Brun, S.E., 1999. *Laboratory experiments on sequential scour deposition and their application to the development of banded vegetation*. CATENA, 37: 147–163.

[8] Bryan, R.B., Govers, G., Poesen, J., 1989. *The concept of soil erodibility and some problems of assessment and application*. CATENA, 16: 393–412.

[9] Bryan, R.B., Shiu-Hung, L., 1981. *Laboratory experiment on the variation of soil erosion under simulated rainfall*. Geoderma, 26: 245–265.

[10] Bultot, F., Coppens A., 1985. *Power of a rainshower*. Hydrological Sciences Journal / des Sciences Hydrologiques, 30(3): 361–369 (in French).

[11] Collinet, J., Valentin, C., 1984. *Evaluation of factors influencing water erosion in West Africa using rainfall simulation*. Challenges in African Hydrology and Water Resources. IAHS Publ., 144.

[12] Diaz-Zorita, M., Duart, G., Grove, H., 2002. *A review of no-till systems and soil management for sustainable crop production in the sub humid and semiarid pampas of Argentina*. Soil & Tillage Research, 65: 1–28.

[13] De Ploey, J., Savat, J., 1968. *Contribution to the study of splash erosion*. Geomorphology, 12: 174–193.

[14] Ellison, W.D., 1947. *Soil erosion studies*. Agricultural Engineering, 28: 402–405.

[15] Erpul, G., Norton, L.D., Gabriels, D., 2002. *Raindrop-induced and wind-driven soil particle transport*. CATENA, 47(3): 227–243.

[16] Farenhorst, A., Bryan, R.B., 1995. *Particle size distribution of sediment transported by shallow flow*. CATENA, 25: 47–62.

[17] Ferro, V., 1998. *Evaluating overland flow sediment transport capacity*. Hydrological Processes, 12(12): 1895–1910.

[18] Fox, D.M., Bryan, R.B., 1999. *The relationship of soil loss by interrill erosion to slope gradient*. CATENA, 38: 211–222.

[19] Gimenez, R., Govers, G., 2002. *Flow detachment by concentrated flow on smooth and irregular beds*. Soil Science Society of America Journal, 66: 1475–1483.

[20] Govers, G., 1985. *Selectivity and transport capacity of thin flows in relation to rill erosion*. Soil Science Society of America Journal, 12: 35–49.

[21] Govers, G., Everaert, W., Poesen, J., Rauws, G., De Ploey, J., Lautridou, J.P., 1990. *A long flume study of the dynamic factors affecting the resistance of a loamy soil to concentrated flow erosion*. Earth Surface Processes and Landforms, 15: 313–328.

[22] Graf, W., Altinakar, M., 2000. *Fluvial hydraulics: Flow and transport phenomena in simple geometry channels*. Presses Polytechniques et Universitaires Romandes (in French).

[23] Guy, B.J., Dickinson, W.T., Rudra, R.P., 1990. *Hydraulics of sediment-laden sheet flow and the influence of simulated rainfall.* Earth Surface Processes and Landforms, 15: 101–118.

[24] Hudson, N., 1995. *Soil Conservation*, (3rd edition). B.T. Batsford, London, 391 pp.

[25] Kilinc, M., Richardson, E.V., 1973. *Mechanics of soil erosion from overland flow generated by simulated rainfall*. Colorado State University, Hydrology Paper, no. 63, Fort Collins, Colorado.

[26] Kinnell, P.I.A., 1991. *The effect of flow depth on sediment transport induced by raindrops impacting shallow flows*. American Society of Agricultural Engineers, 91: 161–168.
[27] Kinnell, P.I.A., 1993. *Runoff as a factor influencing experimentally determined interrill erodibilities*. Australian Journal of Soil Research, 31: 333–342.
[28] Kinnell, P.I.A., 2000. *The effect of slope length on sediment concentrations associated with side-slope erosion*. Soil Science Society of America Journal, 64: 1004–1008.
[29] Kinnell, P.I.A., Cummings, D., 1993. *Soil/slope gradient interactions in erosion by rain-impacted flow*. American Society of Agricultural Engineers, 36: 381–387.
[30] Leguédois, S., Planchon, O., Legout, C., Le Bissonnais, Y., 2005. *Splash projection distance for aggregated soils. Theory and experiment*. Soil Science Society of America Journal, 69(1): 30–37.
[31] Li, G., 2009. *Preliminary study of the interference of surface objects and rainfall in overland flow resistance*. CATENA, 78: 154–158.
[32] Maaliou, A., Mouzai, L., 2018. *The relation between the rainfall erosivity index AI and the hydraulics of overland flow and sediment concentration in sandy soils*. Polish Journal of Soil Science, LI/1: 41–58.
[33] Moussouni, A., Mouzai, L., Bouhadef, M., 2012. *Laboratory experiments: influence of rainfall characteristics on runoff and water erosion*. Journal World Academy of Science, Engineering and Technology, 68: 1540–1543.
[34] Mouzai, L., Bouhadef, M., 2003. *Water drop erosivity: Effects on soil splash*. Journal of Hydraulic Research, 41(1): 61–68.
[35] Nearing, M.A., Bradford, J.M., 1985. *Single Waterdrop Splash Detachment and Mechanical Properties of Soils*. Soil Science Society of America Journal, 49(3): 547.
[36] Ozoko, D.C., Edeani, C., 2015. *Relationship between soil erodibility, rainfall erosivity and geotechnical parameters for soils in gully erosion* sites *in Urualla, Imo State, Nigeria*. International Journal of Science and Research (IJSR), 4(6): 1848–1852.
[37] Pan, C., Shangguan, Z., 2006. *Runoff hydraulic characteristics and sediment generation in sloped grassplots under simulated rainfall conditions*. Journal of Hydrology, 331: 178–185.
[38] Rauws, G., 1987. *The initiation of rills on plane beds of non-cohesive sediments*. In: R. Bryan (ed.), Rill Erosion: Processes and Significance, Catena Supplement, 8: 107–118.
[39] Rauws, G., Govers G., 1988. *Hydraulic and soil mechanical aspects of rill generation on agricultural soils.* Journal of Soil Science, 39: 111–124.
[40] Riezebos, T., Epema, G., 1985. *Drop shape and erosivity.* Part II: *Splash detachment, transport and erosivity indices*. Earth Surface Processes and Landforms, 10(1): 69–74.
[41] Romero, C.C., Stroosnijder, L., Baigorria, G.A., 2007. *Interrill and rill erodibility in the northern Andean highlands*. CATENA, 70(2): 105–113.
[42] Salles, C., Poesen, J., Govers, G., 2000. *Statistical and physical analysis of soil detachment by raindrop impact: Rain erosivity indices and threshold energy*. Water Resources Research, 36(9): 2721–2729.
[43] Schmidt, J., 1993. *Modeling long-term soil loss and landform change*. In: A.J. Parsons, A.D. Abrahams (eds.), Overland flow Hydraulics and Erosion Mechanics, UCL Press, London.
[44] Shih H.-M., Yang, C.T., 2009. *Estimating overland flow erosion capacity using unit stream power*. International Journal of Sediment Research, 24(1): 46–62.
[45] Torri, D., Sfalanga, M., Del Sette, M., 1987. *Splash detachment: Runoff depth and soil cohesion*. CATENA, 14: 149–155.
[46] Truman, C.C., Bradford, J.M., 1993. *Relationships between rainfall intensity and the interrill soil loss-slope steepness ratio as affected by antecedent water content*. Soil Science, 156(6): 405–413.
[47] Young, R.A., Wiersma, J.L., 1973. *The role of rainfall impact in soil detachment and transport*. Water Resources Research, 9(6): 1629–1636.
[48] Zachar, D., 1982. *Soil Erosion. Developments in Soil Science*, vol. 10. Elsevier Science, Amsterdam.